Reaction Chemistry & Engineering

Kinetics Modelling of an Environmentally Friendly Carbamazepine Synthesis via Urea and Iminostilbene in Batch and Continuous Processes

Journal:	*Reaction Chemistry & Engineering*
Manuscript ID	RE-ART-09-2022-000409.R1
Article Type:	Paper
Date Submitted by the Author:	31-Oct-2022

Complete List of Authors:	Kraus, Harrison; University of Maryland at College Park, Department of Chemical and Biomolecular Engineering Acevedo, David; Food and Drug Administration Office of Regulatory Affairs, OPMA Wu, Wei; Food and Drug Administration Office of Regulatory Affairs, DPQR O'Connor, Thomas; Food and Drug Administration Office of Regulatory Affairs, DPQR Mohammad, Adil; Food and Drug Administration Office of Regulatory Affairs, DPQR Liu, Dongxia; University of Maryland at College Park, Department of Chemical and Biomolecular Engineering

ARTICLE

Kinetics Modelling of an Environmentally Friendly Carbamazepine Synthesis via Urea and Iminostilbene in Batch and Continuous Processes

Received 00th January 20xx,
Accepted 00th January 20xx

DOI: 10.1039/x0xx00000x

Harrison F. Kraus[1,2], David Acevedo[2], Wei Wu[2], Thomas F. O'Connor[2], Adil Mohammad[2*], and Dongxia Liu[1*]

[1]Department of Chemical and Biomolecular Engineering, University of Maryland, College Park, MD 20742

[2]Office of Pharmaceutical Quality, Center for Drug Evaluation and Research, U.S. Food and Drug Administration, Silver Spring, Maryland 20993-0002.

*Co-corresponding Authors

Accurate kinetic models for reaction systems allow for improved process understanding and greater quality control, which is particularly beneficial as the pharmaceutical industry shifts from batch to continuous manufacturing (CM). In this work, a first principles kinetic model has been developed for the synthesis of carbamazepine (CBZ) from iminostilbene and urea, starting in a batch reactor and subsequently in a continuous flow reactor. An eco-friendly reaction pathway using urea was selected to avoid the toxic reagents that are typically used for synthesis of CBZ. The kinetic parameters determined from batch reactions were utilized in a MATLAB based kinetic model to simulate the yield for the continuous process. Overall, good agreement between the model prediction and corresponding experimental values were observed for the batch and continuous reaction systems within the full factorial design space. However, the model slightly overpredicted the yield of the continuous reaction system for higher conversion values (>60%) since it did not account for the reverse reaction that can occur at the studied reaction conditions. The use of broken order kinetics was compared with whole number orders, and it was determined that the whole number orders resulted in better agreement at all conversion values for the continuous system.

1 Introduction

Over the past few decades, the pharmaceutical industry has begun to consider the implementation and adoption of continuous manufacturing (CM) technology. The transformation is driven by advantages of this emerging technology such as higher production rates, increased efficiency, smaller footprint, flexible production scale, better quality control, improved system safety, and the possibility of implementing novel synthesis pathways.[1-5] The recent CM approvals of drug products from FDA are primarily focused on drug product manufacturing for solid oral dosage forms, yet the momentum is growing toward further expansion of CM technology to upstream processes including the synthesis of active pharmaceutical ingredients (APIs).[6] Continuous API synthesis can be achieved by flow chemistry using continuous flow reactors. Small scale continuous flow reactors are known to have faster mixing times as well as better temperature control in comparison to batch reactors due to their higher surface area to volume ratio.[7, 8] To maintain the small scale nature of continuous flow reactors, desired throughput rates can be met by 'scaling out' rather than scaling up, meaning increasing the number of reactors not the size of the reactor.[8, 9] Moreover, because continuous systems can run significantly longer than batch systems, effective monitoring and control strategies are crucial for maintaining API quality and minimizing process line stoppages.

One method for ensuring product quality during a CM process is model predictive control (MPC).[10-13] MPC can be used for complex systems such as CM that includes multiple process units and input variables. MPC relies on detailed and accurate knowledge of the system behavior over a range of critical process parameters (CPPs) in order to implement feedforward control.[14, 15] Accurate kinetic models can help to develop a design space, or the range of CPPs that have been shown to

[a] *Address here.*
[b] *Address here.*
[c] *Address here.*
† Footnotes relating to the title and/or authors should appear here.
Electronic Supplementary Information (ESI) available: [details of any supplementary information available should be included here]. See DOI: 10.1039/x0xx00000x

produce assurance of quality.[16] With the advent of quality by design (QbD), the development of design spaces has become more prevalent in recent years.[17-20]

Over the past few years, both mechanistic first principle and empirical models have been developed for a number of API synthesis processes ranging from simple to complex reaction schemes.[21, 22] Computational fluid dynamics and chemical reaction models have been utilized to model reaction pathways as well as to examine the kinetic and mass transfer limitations of API synthesis systems.[23, 24] Design of experiments (DoE) or Monte Carlo simulations have also been used to identify the process parameters that affect the product yield.[19, 23, 25, 26] In some systems, such as the deprotonation of weak Brønsted acids with n-butyllithium, researchers have utilized broken orders to improve model accuracy for systems with non-elementary reaction mechanisms, though this strategy has not been evaluated for API syntheses.[27] Moreover, empirical models such as dynamic response surface methodology or multivariate latent variable models have also been used to predict API yield in systems with complex reaction pathways.[28, 29] First-principle models though represent the physical reaction of the system and can provide mechanistic insights into the process.

The present work describes the development and validation of a first principles kinetic model for an eco-friendly synthesis route for a model API, carbamazepine (CBZ) starting in batch and transferring to continuous flow synthesis. CBZ is a first generation anti-epileptic medication that is also often prescribed for nerve pains such as trigeminal neuralgia.[30] CBZ is on the World Health Organization (WHO) list of essential medicines. As such, the global demand for CBZ is expected to remain high.[31] A few decades ago multiple step routes were used for CBZ synthesis, but more recently single step routes have been developed.[32] This study focuses on reacting iminostilbene (ISB) with urea to produce CBZ, a pathway originally suggested by Vyas et al.[33] The reaction scheme for this chemical pathway is shown in Figure 1. Various other CBZ synthesis pathways have been proposed other the last few decades, which are listed in Table 1. In contrast to these pathways, the reaction with urea was specifically designed to avoid toxic reagents including phosgene, halocyanogens, and cyanide. The patent by Vyas et al. described rather high reaction times (6-8 hours) in batch at 80 – 90°C thus suggesting that continuous flow reaction would not be feasible.[33] However, this current work demonstrates that a much lower residence time can achieve high yield using a slightly elevated temperature (105-110°C).[33] A similar reaction for converting an esterified ISB compound into eslicarbazepine acetate was attempted but failed.[38] The authors claimed that the reaction failed due to the degradation of the starting material. Although they did not specify which reactants degraded, one possibility is the reaction between acetic acid and urea to form acetamide and carbamic acid which further decomposes to carbon dioxide and ammonia. However, literature shows that it is unlikely to have such reaction at the temperatures ranges described by Vyas et al.[39, 40] No kinetic study has been conducted in batch or continuous nor any reactor model developed for this reaction in the literature.

First principles modeling in this work was conducted in MATLAB. The kinetic model which was developed in the batch system was effectively transferred to a continuous plug flow reactor (PFR) model to explore the performance of the continuous system. A full factorial DoE was conducted in the continuous system to examine the model's accuracy given any combination of the key process parameters (KPPs), or parameters that have a significant effect on product yield. The use of broken orders was considered for the developed model against a whole number order kinetic model. Lastly, the developed model was used to examine the reaction pathway

Table 1. CBZ Synthesis routes proposed since 1960.

Patent #	Patent Year	Authors	Reaction Step 1	Reaction Step 2
U.S. 2,948,718[34]	1960	W. Schindler	ISB + Phosgene	Ammonia Add.
German 2,307,174[35]	1973	H. Roehnert, et al.	ISB + Acylisocyanate	Hydrolysis
European 29,409[36]	1981	E. Aufderhaar, et al.	ISB + Halocyanogen	Hydrolysis
European 277,095[37]	1988	G. Acklin, et al	ISB + Hydrogen Cyanide	-
U.S. 6,245,908[33]	2001	K. Vyas, et al.	ISB + Urea	-
U.S. 7,015,322[32]	2006	R. Eckardt et al.	ISB + Alkali Cyanate	-

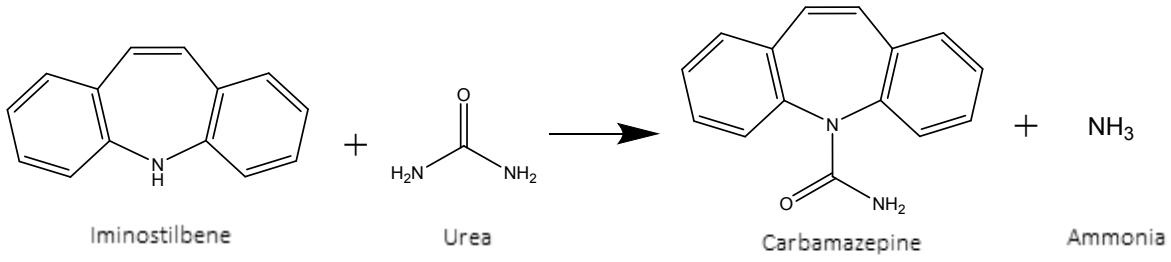

Figure 1. Reaction scheme for the production of Carbamazepine and byproduct ammonia from Iminostilbene and urea

including a potential reverse reaction between CBZ and the ammonium ions.

2 Materials and Methods

2.1 Materials

Iminostilbene (ISB, 97% purity) was purchased from Carbosynth. Urea (99.5% purity), acetic acid (99% purity) and acetonitrile (ACN, 99.9% purity) were acquired from Sigma-Aldrich. Additionally, Ammonium Chloride (99.5% purity) was obtained from Alfa Aesar. MilliQ pure water was used in the work.

2.2 HPLC method

Reaction product solutions were diluted by a ratio of 30 µL of reaction mixture in 900 µL of ACN both sampled using a micropipette (Biohit). These samples were analyzed for ISB conversion and CBZ yield by High-performance Liquid Chromatography (HPLC) (Agilent, 1100 series) equipped with an Zorbax Eclipse XDB-C18 column. The mobile phase consisted of 60 vol% MilliQ pure water and 40 vol% ACN and was maintained at a flow rate of 0.8 ml min-1 at 30°C. A UV-vis detector with detection wavelengths of 211 nm and 254 nm were used for quantifying CBZ and ISB concentrations, respectively.

2.3 Batch reaction for CBZ synthesis

The synthesis of CBZ in the batch reaction was conducted in a 35 mL glass pressure tube reactor (Ace Glass Inc.) that was held in a brass reactor holder as shown in Figure 2 (a). The brass reactor was heated by a stirring hot plate. A glass fiber mat was placed to cover the surface of the brass reactor holder as insulating material to minimize temperature loss/variation. This is represented in Figure 2a and labeled as 'Insulating material'. In a typical batch reaction, 12 mL acetic acid was added into the pressure tube first, followed by addition of desired amount of urea to reach the set concentration (refer to Tables 2-4). The pressure tube reactor was then inserted into the heating block (see Figure 2 (a)) and heated to the desired reaction temperature using an electronic hot plate with a thermocouple and stirring set to 300 rpm (VWR 815). When the heating block reached the desired temperature, the set amount of ISB was added to the mixture. Product samples were collected after the set reaction time, diluted and analyzed by HPLC as detailed in section 2.2.

2.4 Continuous flow reaction for CBZ synthesis

The continuous flow synthesis of CBZ from the mixture of ISB and urea in acetic acid was conducted using an inhouse designed PFR. Figure 2 (b) shows the reactor scheme that contains a syringe pump (Harvard Apparatus, pump 33), 1/16" stainless steel delivery tubing, and 1/4" O.D. (0.18" I.D.) stainless steel tubing as the reaction zone. The total reactor volume was calculated to be 2.2 mL. An oven (Blue M Electric Company, SW-11TA) was used to keep the reaction at desired temperature. To make an easy connection between the PFR reactor inside the oven and the reactant feeding syringe, we connected the syringe needle (outer diameter = 1/16") to a piece of 1/16" stainless steel tubing and then adapted the tubing size to 1/4" stainless steel. The 1/4" stainless steel tubing has larger inner diameter which can allow larger residence time using shorter tubing given the fact that the oven has a small chamber to hold the PFR reactor. The temperature of reaction delivery tubing was maintained at ~40°C using a heating tape (Briskheat, Adjustable Thermostat Control, 120V AC, 288W). In the experiment, the feed solution was prepared by dissolving ISB in acetic acid at room temperature and then adding urea to the solution. ISB has limited solubility in acetic acid at ambient temperature (6 mg/mL), and so to reach higher inlet ISB concentrations, the feed solution was preheated to 40-50°C in batch mode to assist its dissolution. The reactant solution was loaded into a syringe and the syringe was fed into the reactor by the syringe pump at the set flow rate required to obtain the desired residence times. The inlet solution was observed and remained homogeneous throughout each reaction. The reaction effluent was received at the end of the delivery tubing

a) b)

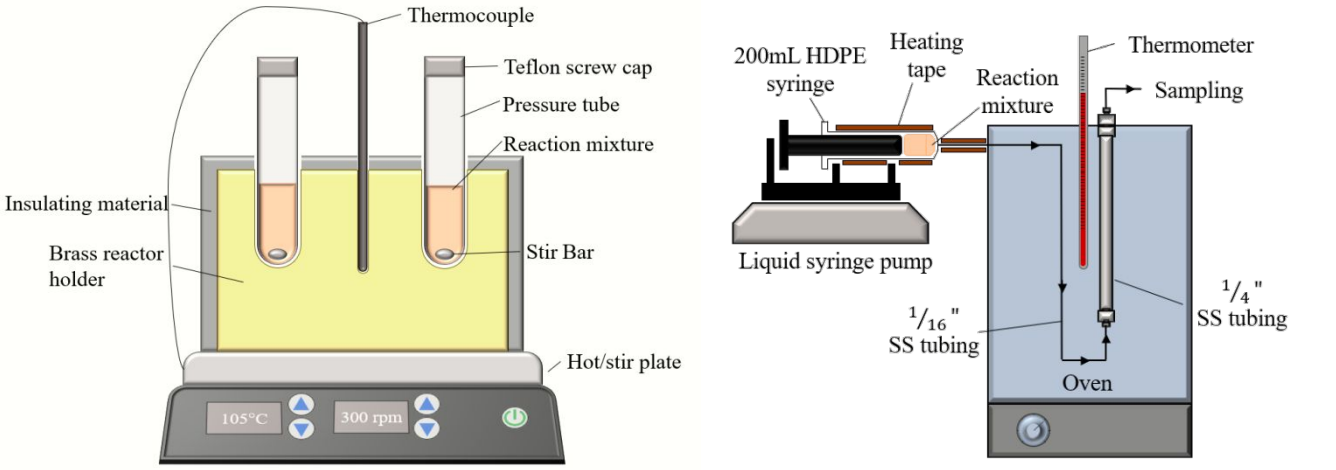

Figure 2. Schematics of experimental set-up for (a) 2 simultaneous batch reactors and (b) continuous plug flow reactor for the synthesis of CBZ from ISB and Urea.

connected to reactor and stored in a glass vial with septum bonded cap for a secure seal to avoid solvent loss. The reaction was run for 1 hour before samples were taken to allow the system to reach steady state. Then 5 product samples were taken at intervals of 12 min, diluted and analyzed by HPLC as detailed in section 2.2. The concentrations of these samples were analyzed to confirm steady state and averaged to determine the yield. Samples of the inlet were also collected before and after reaction completion and it was found that little to no conversion occurred in the syringe (at most 0.9%). To thoroughly examine the continuous synthesis, a two-level full factorial DoE was conducted on four KPPs: the initial concentrations of ISB, urea, residence time, and temperature as summarized in Table 5. The range of the low and high temperature values in this study were a result of limitations with temperature control in the oven, and the upper temperature range was limited by the boiling point of the acetic acid (118℃). The detailed experimental conditions for each continuous flow experiment can be found in Table 6. For some of the continuous flow experiments, the feed solution was allowed to react during the dissolution step resulting in some degree of conversion in the pre-heated feed solution. This pre-conversion was roughly controlled by varying the time allotted for the pre-heating step between 15 and 30 minutes. For experiments with a high ISB inlet concentration at least 15 minutes of heating was required to dissolve all of the material. This pre-conversion step was conducted for two purposes: (a) to make validating the reaction kinetics at higher ISB conversion values (or CBZ yields) feasible; and (b) to formulate kinetics covering higher ISB feed concentrations by avoiding mixing two separate feed solutions. A typical process would involve separate flows of each reactant mixing just prior to the PFR, however, such a scheme in combination with the very limited solubility of ISB would result in a reduced outlet concentration and thus a lower CBZ production rate. The degree of pre-conversion and the inlet CBZ concentrations can be seen in Table 6. Additional continuous flow experiments (Exp 17-24 in

Table 2. Experimental conditions and end product values used for determining reaction orders for ISB and urea at 105℃ in the batch reaction mode.

Exp. #	Reaction time (min)	Initial concentration (mol L^{-1})		CBZ Yield (%)	$[I]_f$ (mol L^{-1})	Reaction rate (mol L^{-1} min^{-1})
		Urea	ISB			
1	10	2.78	0.018	51.6	$8.70 \cdot 10^{-3}$	$9.3 \cdot 10^{-4}$
2	10	2.78	0.020	58.0	$8.40 \cdot 10^{-3}$	$1.2 \cdot 10^{-3}$
3	10	2.78	0.038	35.0	0.025	$1.3 \cdot 10^{-3}$
4	15	2.78	0.039	45.3	0.021	$1.2 \cdot 10^{-3}$
5	20	2.78	0.103	32.7	0.069	$1.7 \cdot 10^{-3}$
6	20	2.78	0.121	32.4	0.082	$2.0 \cdot 10^{-3}$
7	20	2.78	0.133	33.8	0.088	$2.2 \cdot 10^{-3}$
8	20	0.69	0.111	4.1	0.106	$1.95 \cdot 10^{-4}$
9	20	2.08	0.099	27.1	0.072	$1.34 \cdot 10^{-3}$
10	8	3.70	0.086	32.1	0.058	$3.44 \cdot 10^{-3}$
11	5	4.17	0.084	19.4	0.068	$3.27 \cdot 10^{-3}$
12	5	5.56	0.099	34.5	0.065	$6.83 \cdot 10^{-3}$

Table 3. Experimental conditions and end product values used of the validation reactions performed at 105℃ in the batch reaction mode.

Exp. #	Reaction time (min)	Initial concentration (mol L^{-1})		Experimental Yield (%)	Model Yield (%)
		Urea	ISB		
1	6	2.78	0.183	7.9	10.9
	20			30.7	33.4
	40			67.3	59.2
	60			88.0	78.2
	90			93.4	95.4
	120			95.1	100.0
	140			95.0	100.0
2	5	3.48	0.117	27.6	18.5
	15			50.7	49.4
	25			84.7	72.6
	35			89.6	88.7
	45			92.7	97.8
	70			93.5	100.0
3	20	3.70	0.086	75.7	76.6
4	20	4.17	0.084	90.4	90.0
5	20	5.56	0.099	97.1	100.0

Table 4. Experimental conditions and end product values used for determining Arrhenius parameters at temperatures from 95-112℃ in the batch reaction mode.

Exp. #	Reaction time (min)	Reaction temperature (℃)	Initial concentration (mol L^{-1})		CBZ Yield (%)	k (from MATLAB) ($L^{1.29}$ $mol^{-1.29}$ min^{-1})
			Urea	ISB		
1	6	95	2.78	0.024	14.4	$4.44 \cdot 10^{-4}$
2	6	100	2.78	0.022	28.5	$8.74 \cdot 10^{-4}$
3	6	105	2.78	0.021	41.9	$1.31 \cdot 10^{-3}$
4	6	108	2.78	0.022	67.4	$2.40 \cdot 10^{-3}$
6	4	105	2.78	0.023	32.3	$1.52 \cdot 10^{-3}$
7	4	110	2.78	0.024	53.1	$2.78 \cdot 10^{-3}$
8	4	112	2.78	0.024	53.1	$2.80 \cdot 10^{-3}$

Table 5. High and low values for continuous flow reactor full factorial study.

	Low Value	High Value
Initial ISB Concentration (mol L^{-1})	$2.40\text{-}2.60 \cdot 10^{-2}$	$4.11\text{-}5.32 \cdot 10^{-2}$
Initial Urea Concentration (mol L^{-1})	1.390	2.664
Residence Time (min)	6	12
Temperature (℃)	95-100	105-110

Table 6. Experimental conditions used for continuous flow reactor experiments alongside experimentally measured and model predicted CBZ yields.

Exp. #	Inlet Concentration (mol L^{-1})			Temp. (℃)	Residence time (min)	Pre-Conversion (%)	Experimental Outlet Yield (%)	BO Model Outlet Yield (%)	WNO Model Outlet Yield (%)
	ISB	Urea	CBZ						
1	$2.47 \cdot 10^{-2}$	1.39	0	99.3	6	0.0	11.3	8.2	8.2
2	$5.21 \cdot 10^{-2}$	1.39	$1.17 \cdot 10^{-3}$	97	6	2.2	10.7	6.3	8.6
3	$2.47 \cdot 10^{-2}$	1.39	0	107.3	6	0.0	15.9	20.2	18.3
4	$4.14 \cdot 10^{-2}$	1.39	$7.98 \cdot 10^{-3}$	104.4	6	16.2	27.6	25.4	27.8
5	$2.40 \cdot 10^{-2}$	2.664	$2.78 \cdot 10^{-4}$	100.1	6	1.1	28.7	30	29.9
6	$3.17 \cdot 10^{-2}$	2.664	$9.44 \cdot 10^{-3}$	97.8	6	23.0	36.7	38.1	41.2
7	$2.23 \cdot 10^{-2}$	2.664	$2.47 \cdot 10^{-3}$	107.7	6	10.1	66.5	68.2	58.5
8	$3.76 \cdot 10^{-2}$	2.664	$8.91 \cdot 10^{-3}$	104.7	6	19.2	52.3	49.9	54.2
9	$2.54 \cdot 10^{-2}$	1.39	0	95.8	12	10.0	18.3	10.7	11
10	$5.29 \cdot 10^{-2}$	1.39	$4.15 \cdot 10^{-4}$	96.5	12	0.8	13	8.5	12.7
11	$2.55 \cdot 10^{-2}$	1.39	0	106.2	12	0.0	30	33.8	30.3
12	$5.17 \cdot 10^{-2}$	1.39	$6.97 \cdot 10^{-5}$	107.5	12	0.1	28.3	27	34.1
13	$2.58 \cdot 10^{-2}$	2.664	$2.16 \cdot 10^{-4}$	97.9	12	0.8	44.4	42.2	42.3
14	$3.22 \cdot 10^{-2}$	2.664	$8.92 \cdot 10^{-3}$	98.6	12	21.7	52.4	53.1	56.3
15	$2.53 \cdot 10^{-2}$	2.664	$1.91 \cdot 10^{-4}$	109	12	0.7	71.9	99.8	83.4
16	$4.65 \cdot 10^{-2}$	2.664	$1.46 \cdot 10^{-3}$	106.9	12	3.1	62.6	75.3	76.7
17	$2.40 \cdot 10^{-2}$	2.664	$2.78 \cdot 10^{-4}$	96.3	6	1.1	16.8	20.3	21.4
18	$2.48 \cdot 10^{-2}$	2.664	$4.20 \cdot 10^{-4}$	108.4	6	1.7	60.9	66.7	57.6
19	$7.67 \cdot 10^{-3}$	2.647	$1.68 \cdot 10^{-2}$	107.8	6	68.7	83	98.5	85.6
20	$1.57 \cdot 10^{-2}$	2.654	$9.61 \cdot 10^{-3}$	106.2	12	37.9	82.4	99.4	83.6
21	$3.74 \cdot 10^{-2}$	2.664	$9.55 \cdot 10^{-3}$	105.1	12	20.4	76.8	76.4	75.6
22	$3.74 \cdot 10^{-2}$	2.664	$9.37 \cdot 10^{-3}$	105.6	9	20.0	62.9	67.2	68.7
23	$4.92 \cdot 10^{-2}$	2.664	$1.50 \cdot 10^{-3}$	105.3	9	3.0	43.8	51.8	60.8
24	$4.07 \cdot 10^{-2}$	2.664	$7.19 \cdot 10^{-3}$[a]	107.4	30	1.1	85.7	100	98

[a] This conversion did not occur while in contact with air but rather while the feed solution was being heated in the syringe since this reaction was run for 6 hours to allow the system to reach steady state due to the high residence time

Table 6) were manually designed to focus on higher conversion and to better understand the effects of pre-conversion.

2.5 Model Development

All first principles modeling work was conducted in MATLAB 2021b environment. The ordinary differential equation of the reaction rate (Eq. 1) was solved using ODE45 with a step size of 0.5 minutes. In order to develop a model kinetic equation for this reaction system, the following rate equation was used,

$$\frac{d[C]}{dt} = \boldsymbol{k}(\boldsymbol{T})[\boldsymbol{I}]^{\boldsymbol{i}}[\boldsymbol{U}]^{\boldsymbol{u}} \quad (1)$$

where *[C]*, *[I]*, and *[U]* are the molar concentrations of CBZ, ISB, and urea, respectively; t is time, *i*, and *u* are the reaction orders; and $\boldsymbol{k}(\boldsymbol{T})$ is defined by the Arrhenius equation:

$$k(T) = Ae^{-\frac{E_a}{RT}} \quad (2)$$

where *T* is the temperature of the system, *R* is the universal gas constant in J mol^{-1} K^{-1}, and E_a and *A* are the activation energy and the pre-exponential factor, respectively.

For modeling the continuous flow system, the full factorial study was analyzed using JMP software to determine which input variables had significant effect on the PFR conversion. An empirical model was also developed from this analysis for comparison with the first principles model. For the first principles model of the PFR, the kinetic equation is similar to the batch reactor equation except that conversion in a PFR occurs along the reactor length (*z*) rather than with time (*t*). This can be expressed as,

$$\frac{d[C]}{dz} = \frac{k(T)[I]^i[U]^u}{v} \quad (3)$$

where v is the linear flow rate of the feed solution. The linear flow rate was calculated using the inner radius of the PFR in conjunction with volumetric flow rate of the feed solution. For the continuous reactions ODE45 solved the system using 100 segments along the reactor length not including the $1/16$-inch stainless steel delivery tubing. Nonlinear least-squares curve fitting (i.e., Lsqnonlin function in MATLAB) was also used, as needed, to refine kinetic parameter values.

3 Results and Discussion

3.1 Rate equation determination from kinetics study in batch reactions

The input conditions used to determine reaction kinetics are summarized in Table 2 along with the experimentally measured CBZ yields. The reaction orders were initially determined by running batch reactions at relatively low conversions where the reaction rate is pseudo-linear and not affected by the decreasing reactants concentration. In order to determine the reaction order with respect to ISB, batch order experiments were conducted in which the concentration of urea was kept in excess of ISB. The initial concentration of ISB, represented by $[I]_i$, was varied from 0.018 to 0.133 mol L^{-1} (refer to Exp 1-7 in Table 2). The following equation is obtained by linearizing Eq. (1):

$$\ln\left(\frac{\Delta[C]}{\Delta t}\right) = \mathbf{i}\cdot\ln([I]) + \mathbf{u}\cdot\ln([U]) + \ln(k(T)) \quad (4)$$

where *Δ[C]* is the difference in the concentration of CBZ from the start to the end of the reaction, and *Δt* is the total reaction run time. Since urea concentration *[U]* was nearly constant in these experiments, plotting $\ln\left(\frac{\Delta[C]}{\Delta t}\right)$ vs. $\ln([I]_i)$ yielded a linear relationship with *i* as the slope. As shown in Figure 3(a-b), the reaction rate ($r = \frac{\Delta[C]}{\Delta t}$, mol L^{-1} min^{-1}) increased with ISB concentration,

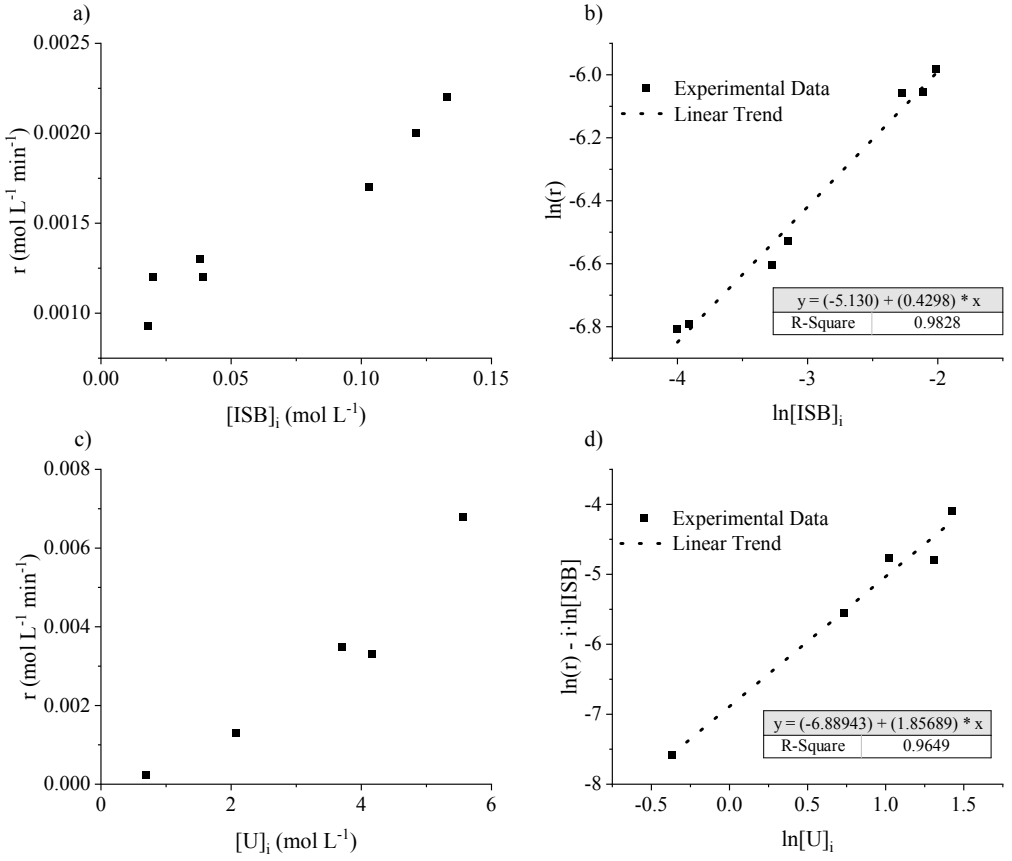

Figure 3. Dependence of CBZ production rate on ISB concentration at a fixed urea concentration of 2.78 mol L^{-1} (a) and on urea concentration at a fixed ISB concentration of ~0.096 mol L^{-1} (c). (b) and (d) show the corresponding log-log plots based on the linearized power rate equation of these data sets. The dashed lines in (b) and (d) represent predictions from Eq. 4. (105°C, 12 mL acetic acid, 0.018-0.133 mol L^{-1} ISB, 0.69-5.56 mol L^{-1} Urea).

and the slope of the linearized graph yielded the ISB order value of 0.430 (R^2 of 0.983).

Owing to the very low solubility of ISB in acetic acid, a similar experiment scheme could not be used to determine the reaction order for urea. To overcome this limitation, a nearly constant ISB concentration (lower than urea) was maintained while the initial concentration of urea, $[U]_i$, was varied from 0.69 to 5.56 mol L^{-1} throughout the experiments (refer to Exp 8-12 in Table 2). Since ISB concentration cannot be assumed to be constant over the reaction period, the average ISB concentration value (denoted as $[I]_{avg}$) between the initial $[I]_i$ and the final ISB concentration, $[I]_f$, was used in the reaction order calculation, *u* in Eq. (1). Therefore, plotting $\ln\left(\frac{\Delta[C]}{\Delta t}\right) - i \cdot \ln([I]_{Avg})$ vs. $ln([U])$ in Eq. (4) yielded a linear relationship with *u* as the slope. Figure 3(c-d) shows that the reaction rate increases with urea concentration, and the slope of the linearized graph yields the urea order value of 1.857 (R^2 of 0.965). The observed high R^2 values further justifies the linear relationship assumption.

The rate constant was also calculated from each plot. According to equation 4, the y-intercept of each graph will give $\ln(k) + u \cdot \ln([U])$ and $\ln(k)$ for the ISB and urea plots, respectively. The k parameter for each plot was found to be $8.86 \cdot 10^{-3}$ and $1.01 \cdot 10^{-2}$ $L^{1.29}$ $mol^{-1.29}$ min^{-1} for the ISB and urea plots, respectively. Both values were tested for modeling all the data available at 105°C and it was determined that $1.01 \cdot 10^{-2}$ $L^{1.29}$ $mol^{-1.29}$ min^{-1} gave more accurate results possibly because this value came from the modified linearization. The rate equation determined from the kinetics in the batch reactions is therefore

$$\frac{d[C]}{dt} = 0.0101 \frac{L^{1.29}}{mol^{1.29} \cdot min} [I]^{0.430}[U]^{1.857}. \quad (5)$$

3.2 Batch reaction model validation and temperature dependence

To verify the kinetic model derived from the batch reaction conditions for CBZ synthesis, five validation experiments were designed (See Table 3). The first two (Exp. 1 and 2 in Table 3) had varying ISB and urea concentrations and allowed to reach nearly full conversion in order to test the obtained kinetic parameters over a range of initial reactant initial concentrations and conversion values.

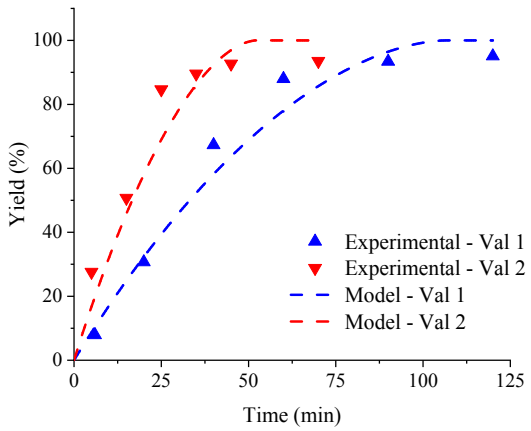

Figure 4. Comparison between experimental and model predicted CBZ production as a function of reaction time in two batch validation reaction conditions. (Experimental #1 condition: 105°C, 12 mL acetic acid, 0.183 mol L^{-1} ISB, 2.78 mol L^{-1} Urea; Experimental #2 condition: 105°C, 12 mL acetic acid, 0.117 mol L^{-1} ISB, 3.48 mol L^{-1} Urea).

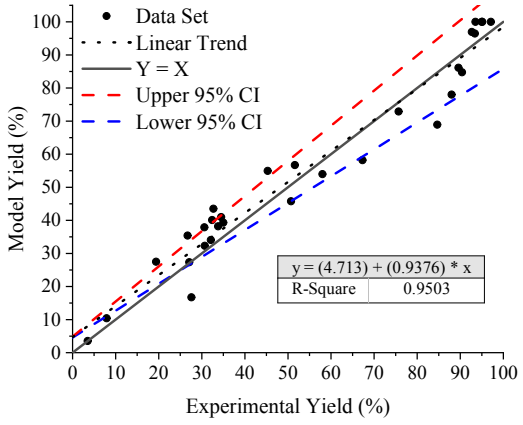

Figure 5. Comparison of the CBZ yields predicted by the batch reaction model to the experimentally measured yields for all batch experiments (the corresponding experimental conditions are included in Tables 2 and 3).

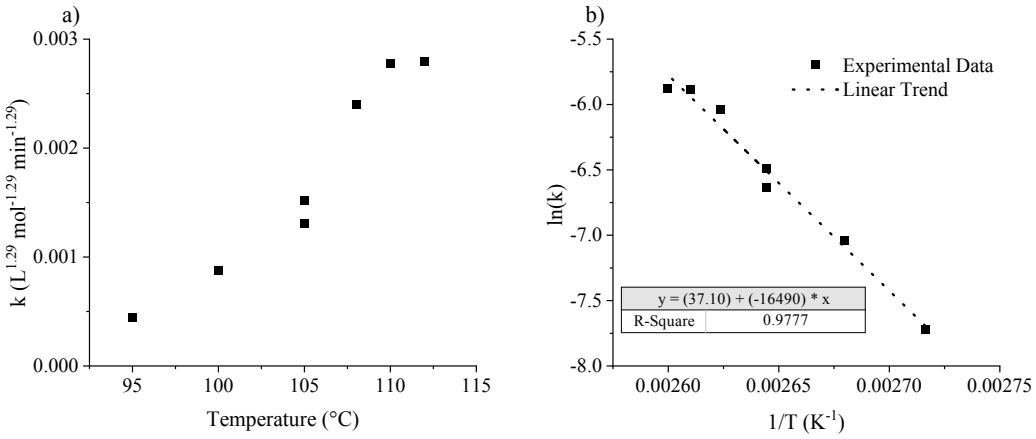

Figure 6. CBZ production rate constant as function of reaction temperature (a) alongside the Arrhenius plot of this data set (b) in batch reaction mode (the corresponding experimental conditions are included in Table 4).

Experiments 3-5 were performed with high concentration of urea to focus specifically on the model's ability to predict yield at high conversions. Validation run 1 was started with initial ISB and urea concentrations of 0.183 mol L^{-1} and 2.78 mol L^{-1}, respectively. Validation run 2 started with initial concentrations of 0.117 mol L^{-1} and 3.48 mol L^{-1}. As shown in Figure 4, the kinetic model showed a good agreement with the experimental results, although it slightly underpredicted at moderate to high conversions (e.g., 60-85%), and slightly over predicted at higher conversion (e.g., >85%). A comparison between yields of predicted (model) and measured (experimental) data for the batch reactions is shown in Figure 5, with dotted line indicating the 95% confidence intervals of the predicted yields. Most data points fell within the confidence intervals with the exception of a few data points that corresponds to low conversion.

After the kinetic model was determined at a fixed temperature, its dependence on reaction temperature was further measured by running batch reactions with 0.024 mol L^{-1} ISB and 2.78 mol L^{-1} urea for 4-6 minutes with temperatures ranging from 95 to 112°C (Exp 1-8 in Table 4). Lower residence times were used for higher temperatures to maintain low conversion. Then, *k* values were calculated for each temperature in MATLAB using the previously determined power law exponent values. The relationship between *k* and temperature is shown in Figure 6 (a). As expected, the *k* value increases with increasing reaction temperature. The relation between the rate of reaction and temperature was quantified by Arrhenius equation (Eq. 2). As shown in Figure 6 (b), plotting $\ln(k)$ vs. $1/T$ yields the activation energy (E_a) and pre-exponential factor (A) values of 137.1 kJ mol^{-1} and 1.297E+16 $L^{1.29}$ $mol^{-1.29}$ min^{-1}, respectively. The same four kinetic parameters (i.e., *i*, *u*, *A* and E_a), from batch experiments, were then employed in modeling the continuous synthesis of CBZ, as discussed in section 3.3.

3.3 Continuous CBZ synthesis and modelling

Table 7. JMP Effects Summary on the PFR conversion for the full factorial study with 4 KPPs effect and their two-way interactions

Source	LogWorth	PValue
Urea	4.811	0.00002
Temperature	4.050	0.00009
Residence Time (RT)	3.653	0.00022
ISB	2.826	0.00149
Urea*Temp	2.630	0.00234
ISB*Urea	1.901	0.01257
Urea*RT	1.347	0.04493
Temp*RT	1.174	0.06706
ISB*RT	0.435	0.36764
ISB*Temp	0.180	0.66057

Table 8. JMP Parameters Estimates for the reduced empirical model using 4 KPPs effect and the Urea – Temperature two-way interaction terms

Term	Estimate	Std Error	t Ratio	Prob>|t|
Intercept	-216.8	33.21	-6.53	<.0001*
ISB	-518.2	150.0	-3.45	0.0062*
Urea	19.65	2.184	9.00	<.0001*
Temperature	1.979	0.3149	6.28	<.0001*
Residence Time	2.410	0.4638	5.20	0.0004*
(Urea-2.027) *(Temp-102.3)	1.543	0.4943	3.12	0.0108*

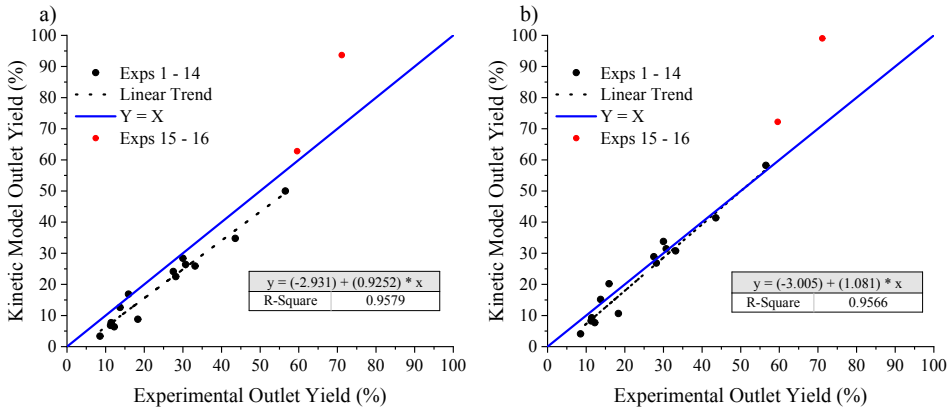

Figure 8. Comparison of the CBZ yield predicted by the first-principles PFR model to the experimentally measured yield for all 16 full factorial experiments using: (a) kinetics obtained from batch reaction, and (b) kinetics obtained from running lsqnonlin on continuous experiments 1-14) (the corresponding experimental conditions are included in Table 6).

To implement continuous synthesis of CBZ, a PFR was used as shown in Figure 2b. The experimental conditions and measured outlet yields of the continuous synthesis full factorial study are shown in Table 6 (exp. 1 – 16). JMP software was utilized for data analysis to determine which KPPs had the greatest effect on the CBZ yield. The effect summary of the four KPPs (ISB, urea inlet concentration, temperature, and residence time) are shown in Table 7. The LogWorth values in this table show that the effect terms of all four KPPs were statistically significant, with urea concentration being the most significant, followed by temperature, residence time, and ISB concentration. This finding aligns with the first principles batch model since the high urea reaction order and activation energy indicate that any change in urea concentration or temperature would have considerable effect on the yield. The low ISB reaction order in the batch model indicates that changes in ISB concentration have the least effect on the yield. Table 7 also demonstrates that the two-way interaction between temperature and urea concentration is also significant. This effect is not expected and what it might represent chemically is unclear.

An empirical model was subsequently constructed in JMP using only the effects shown to be significant in Table 7. Table 8 shows the parameter estimates for each term in this empirical model. The resulting model equation can be expressed as:

$$\boldsymbol{conversion} = -\mathbf{216.8} - \mathbf{518.2}[\boldsymbol{I}] + \mathbf{19.65}[\boldsymbol{U}] + \mathbf{1.979}\boldsymbol{T} + \mathbf{1.543}\boldsymbol{\tau} + ([\boldsymbol{U}] - \mathbf{2.027})(\boldsymbol{T} - \mathbf{102.3}) \quad (6)$$

where *conversion* is the percent of ISB from the feed that converted to CBZ in the PFR, $\boldsymbol{\tau}$ is residence time in minutes, and T is the temperature in °C. Note that the ISB coefficient is negative, which is expected since ISB is the limiting reagent and therefore an increase in ISB will decrease the yield. A comparison between experimentally measured conversion and conversion predicted by this empirical model for all continuous flow experiments can be seen in Figure 7. This Figure demonstrates that the empirical model gives good agreement with the continuous flow reaction data for all the full factorial experiments except for exp. 2 (Table 6), for which it underpredicts yield. However, the model overpredicts yield for some of the validation experiments that had high experimental yield, the conditions of which lie outside those tested in the full factorial study. This is an expected drawback of the empirical model approach. Moreover, the empirical model cannot give insight as to why it fails for certain experiments and not for others. A first principles model

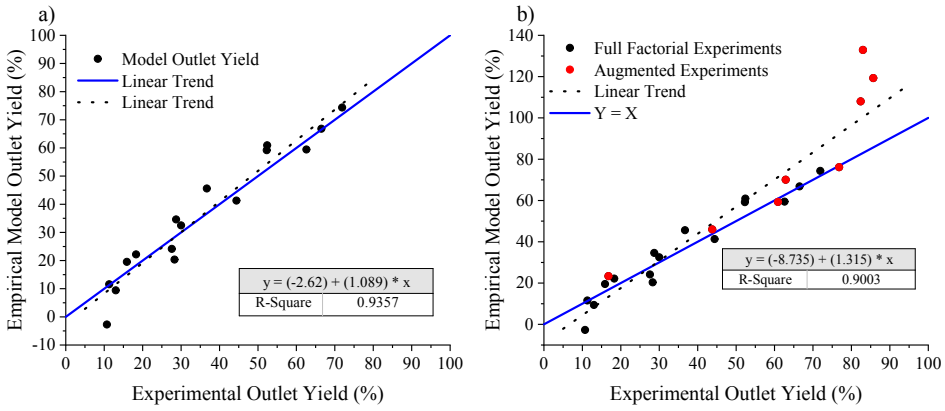

Figure 7. Comparison of the CBZ yield predicted by the empirical model to the experimentally measured yield for (a) the full factorial experiments, and (b) all continuous flow experiments with experiments from the augmented portion of the design of experiments indicated in red.

on the other hand handles changes in the reaction conditions more accurately and provides greater insight into any model inaccuracies.

First principles modeling of the continuous flow synthesis of CBZ was conducted by using the kinetic parameters obtained from the batch reaction mode and the reaction design equation of a PFR. It was assumed that the reaction ran under steady state condition without heat and mass transfer resistance, and in the absence of reverse and side reactions. The reactor dimensions were kept the same as experimental setup shown in Figure 2 (b). The predicted and experimentally measured yield values are shown in Figure 8 (a). A relatively good linear relationship can be observed for the model prediction and corresponding experiments 1 to 14, whereas the kinetic model seems to slightly overpredict experiments 15 and 16. The observed over-prediction behavior of the model at higher conversion is discussed in more detail later.

For comparison between the batch continuous systems, the values of A and E_a were recalculated via a non-linear least squared error solver in MATLAB (lsqnonlin function) by minimizing the error in the yield for Exp 1-14 of Table 6. Only the error of these 14 experiments were minimized since they fit the linear trend [Figure 8 (a)]. Here, the i and u values were held constant at the values determined from the batch reactions. After recalculating A and E_a, the value of A remained unchanged while E_a was recalculated to be 136.6 kJ mol^{-1}, only a -0.44% difference from the batch value. This small difference could be a result of the PFR not quite reaching the observed temperature of its surroundings. However, it still demonstrates good agreement between the batch and continuous Arrhenius model parameters. The experimental yield of the full factorial experiments in comparison with the model predicted yield using the re-calculated E_a value is shown in Figure 8 (b). This revised model shows the same linear trend in Exp 1-14 and gives better agreement with the experimental values. The linear trendlines in both Figures 8 (a) and 8 (b) did not include Exp 15-16 as they did not fit the trend of the rest of the data.

The model predicted yield values for all continuous reactions can be found in Table 6 under the broken order (BO) model heading. Figure 9 (a) shows the comparison between the experimental and model yield values for all continuous reactions using the recalculated E_a value and the *A*, *i*, and *u* values obtained from the batch study. From this Figure, we see that the model gives good agreement with the experimental values up to 60% reaction conversion. The observed overestimation at higher conversions is fairly common in modeling such systems.[23] Nevertheless, one benefit of first principles modeling is that the model can give insights into the system that empirical models cannot. For instance, in this case, the over-prediction at yields above 60% could be a result of either ammonia evolution or a reverse reaction. Had ammonia evolved into the gas phase in the PFR the newly formed gas would push the liquid phase out of the reactor faster thus reducing the residence time. For reactions that had undergone greater yield, more ammonia would form thus reducing the residence time more and causing the experimental yield to be lower than predicted. It is also possible that the ammonia did not escape into the gas phase but remained in the liquid as ammonium and contributed to a reverse reaction that was not considered in the first principles model equation. To verify the presence of a reverse reaction, a batch reaction was run starting with 14.7 mg mL^{-1} CBZ, 3.32 mg mL^{-1} NH_4Cl, and 79.78 mg mL^{-1} urea in 12 mL acetic acid at 110°C. This simulates the product solution of continuous experiment 7 (assuming 100% conversion). This reaction was run for ~6 hours to let it reach equilibrium. Upon HPLC analysis it was determined that the solution underwent 7.45% conversion from CBZ to ISB. Modeling this reverse reaction is outside of the scope of this work, but its occurrence could explain why the model overpredicts yield at high conversions. The addition of ammonium acetate shoed the same effect as that of the ammonium chloride in the reverse reaction.

Another question that this study sought to answer was why the reverse reaction was more prevalent in the continuous system than it had been in the batch system. Comparing Figure 5 with Figure 9 (a), one can see that the model does not over-predict for batch reactions nearly as much as it does for the continuous reactions. From this data, it was hypothesized that in the batch system, ammonia was able to escape into the air in the pressure tube reactor and was not present to feed the reverse reaction. If this hypothesis were true, then one would expect the model to be more accurate for continuous reactions that underwent greater pre-conversion (>10%) while in contact with air since ammonia could escape during the pre-conversion step. Therefore, the model error for experiments with less than 5% pre-conversion and for those with greater than 10% pre-

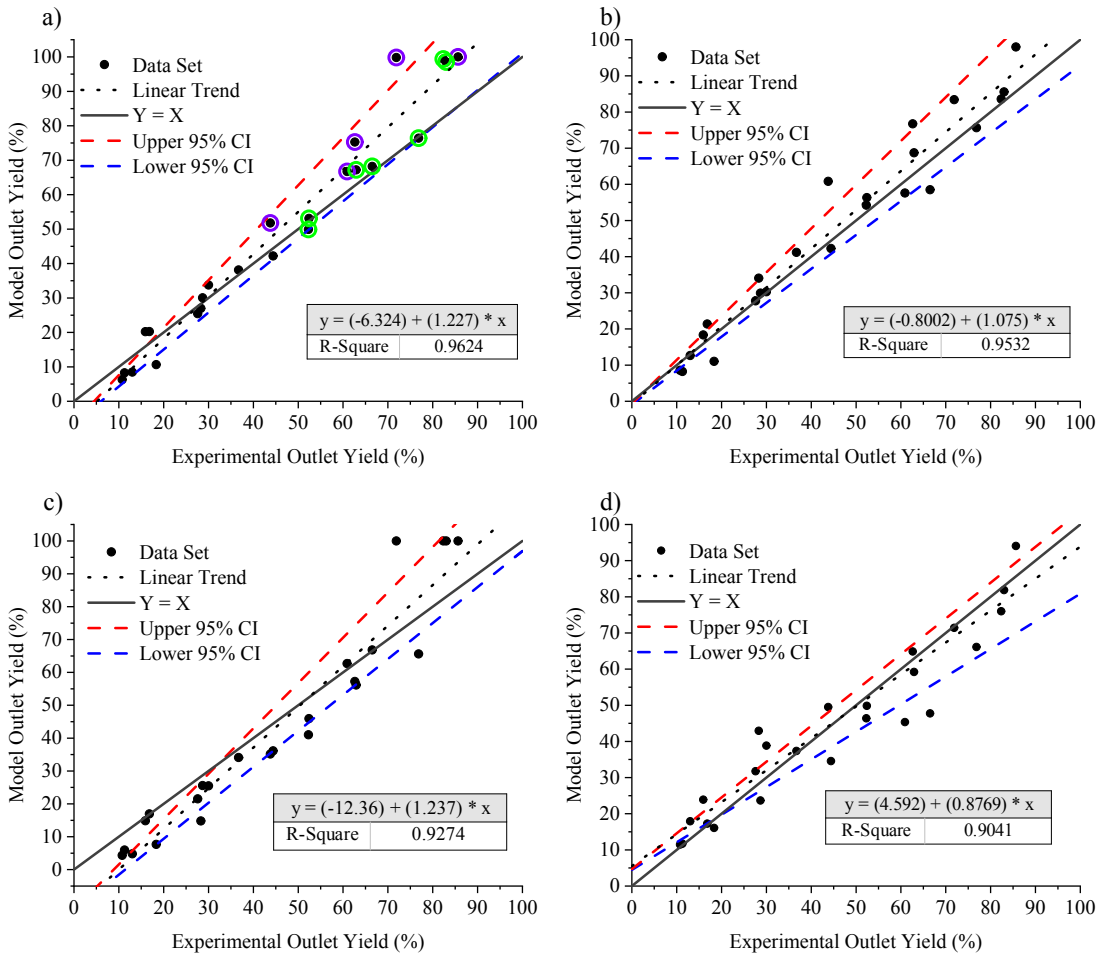

Figure 9. Comparison of the CBZ yield predicted by the continuous reaction model to the experimentally measured yield for all PFR experiments using broken reaction orders (a), and integer reaction orders pairs i = 1, u = 2; i = 0, u = 2; i = 1, u = 1 (b-d, respectively). In (Figure 9a), points with a green outline underwent >10% conversion with exposure to air, while points with a violet outline underwent <5% conversion with exposure to air (the corresponding experimental conditions are included in Tables 6).

conversion were compared (only considering reactions with over 50% yield since that is where the over-prediction error existed). For the five experiments whereby the feed solution underwent <5% pre-conversion, the model average error was 13.7% (data points are marked by violet circle outlines in Figure 9 (a)). On the other hand, for the seven experiments whereby the feed solution underwent >10% pre-conversion, the model average error was 5.2% (marked by green circle outlines in Figure 9 (a)). I.e., the overprediction error was less ($p = 0.093$) for experiments with greater than 10% pre-conversion while in contact with air.

3.4 Broken vs. whole number order kinetics for continuous reaction mode

In order to further improve the accuracy of the model, whole number orders (WNOs) were considered for both urea and ISB in place of the experimentally determined broken orders (BOs). It is possible that the BOs measured in batch were not completely accurate since these values were found using low to medium CBZ yield values (see Table 2) that may not have represented the exact initial reaction rates. Therefore, three WNO pairs (i = 1, u = 2; i = 0, u = 2; and i = u = 1) were considered, and the model prediction accuracy of these three models were compared against the BO model. For each WNO pair, the activation energy and pre-exponential factor were recalculated, using lsqnonlin MATLAB function, on the reaction yields of Exp 1-14, in Table 6. Only the first 14 experiments of the full factorial study were considered here because they showed a linear relationship when using the batch measured parameters indicating that they were not as affected by the reverse reaction (as seen in Figure 8 (a)). Exp 15 – 24 from Table 6 were utilized for model validation. Most of these validation reactions had experimentally high yields. These were utilized to examine how accurate a model that did not consider the reverse reaction would be for experiments that were measured to have high yields.

Figure 9 (a-d) shows the comparison between the accuracy of the BO model and the WNO model on all continuous reaction data as well as the 95% upper and lower confidence intervals for all models. From Figure 9 (a-d), it can be seen that of all the order pairs considered (both broken and whole), the WNO model with i= 1, u= 2, and re-calculated 126.5 kJ mol^{-1} activation energy and 4.14E+15 L^2 mol^{-2} min^{-1} pre-exponential factor provides the most accurate overall trend. This WNO model resulted in a decrease in the overall average error from 6.27% in the BO model to 4.87% in the WNO model. It is worth mentioning that although the model prediction is improved using the WNO model, there is still a slight over-estimation of yield at high conversion even for the best WNO model. Moreover, this model (Figure 9(b)) may be less consistent than the BO model (Figure 9(a)), since it shows more points that lie outside of the 95% confidence interval. As was the case for the in the BO model, these errors in the WNO model are likely due to the reverse reaction that was not accounted for in either model.

3.5 Reverse reaction modeling

Upon verification of the reverse reaction with ammonium in the PFR system, a simple reaction network was suggested, which can be seen in figure 10(a). This network involves the intermediate reaction step in which urea breaks down to form cyanate and ammonium (Rxn 1). The cyanate subsequently reacts with ISB to form CBZ (Rxn 3). The intermediate reaction has been suggested to be reversible in the literature (Rxn 2).[41] This fits the data from this study because an increased amount of ammonium in the system will shift this equilibrium toward urea decreasing the concentration of cyanate and thus decreasing the rate of Rxn 3. It has also been observed that CBZ will break down to form ISB in acetic acid without the presence of any other reagents, and so reaction 4 has been included in the network.

To model this reaction network each reaction was assumed to be first order with respect to each reactant. The rate constants were expressed using the Arrhenius equation. These can be expressed as

$$\boldsymbol{r_1 = k_1(T)[U]} \quad (7)$$

$$\boldsymbol{k_1(T) = A_1 e^{-\frac{E_{a_1}}{RT}}} \quad (8)$$

$$\boldsymbol{r_2 = k_2(T)[Cy][A]} \quad (9)$$

$$\boldsymbol{k_2(T) = A_2 e^{-\frac{E_{a_2}}{RT}}} \quad (10)$$

$$\boldsymbol{r_3 = k_3(T)[Cy][I]} \quad (11)$$

$$\boldsymbol{k_3(T) = A_3 e^{-\frac{E_{a_3}}{RT}}} \quad (12)$$

$$\boldsymbol{r_4 = k_4(T)[C]} \quad (13)$$

$$\boldsymbol{k_4(T) = A_4 e^{-\frac{E_{a_4}}{RT}}} \quad (14)$$

where $\boldsymbol{A_j}$ and $\boldsymbol{E_{aj}}$ are the Arrhenius parameters that must be calculated, and [Cy] and [A] are the concentrations of cyanate and ammonium (mol/L), respectively. Based on these reaction rates, the

a)

Reaction network:

Rxn 1: Urea → Cyanate + Ammonium

Rxn 2: Cyanate + Ammonium → Urea

Rxn 3: Cyanate + ISB → CBZ

Rxn 4: CBZ → Cyanate + ISB

b)

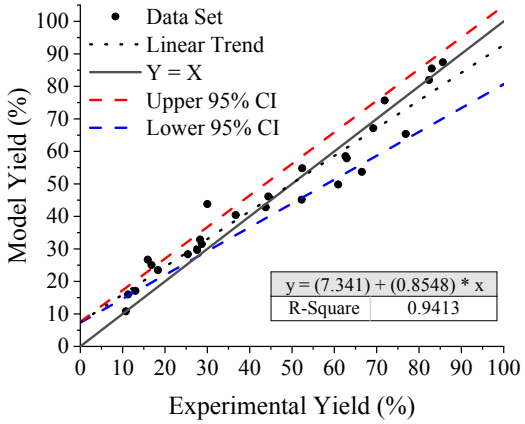

Figure 10. (a) Reaction network involving the reverse reaction with ammonium and (b) comparison of the CBZ yield predicted by the reaction network model to the experimentally measured yield for all PFR experiments including the 2 reactions conducted to verify the reverse reaction.

change in the concentrations of the reactants along the length of the PFR can be expressed as

$$\frac{d[U]}{dz} = \frac{r_2 - r_1}{v} \quad (15)$$

$$\frac{d[Cy]}{dz} = \frac{r_1 - r_2 - r_3 + r_4}{v} \quad (16)$$

$$\frac{d[A]}{dz} = \frac{r_1 - r_2}{v} \quad (17)$$

$$\frac{d[I]}{dz} = \frac{r_4 - r_3}{v} \quad (18)$$

$$\frac{d[C]}{dz} = \frac{r_3 - r_4}{v} \quad (19)$$

which were solved using ODE45 in MATLAB with similar methodology to that described in section 2.5. The Arrhenius parameters values were determined by minimizing the error on the yield for all PFR experiments including the two run for studying the reverse reaction using MATLAB function lsqnonlin. These values can be seen in table 9. During the optimization process, the A value for reaction 4 was calculated to be <100 so this reaction was eliminated from the final model. The high activation energy of reaction 1 shows that the decomposition of urea is the rate limiting step. Figure 10(b) shows the accuracy of this model for all PFR experiments. This figure shows that the reaction network model tended to overpredict yield at low yields and underpredict at high yields. This could be a result of overestimating the significance of the reverse reaction. Some limitations of this model include the first order assumption for all reactants, and the assumption that the feed contained no ammonia or cyanate even when some pre-conversion had occurred. This second assumption was necessary as HPLC cannot measure the concentration of either of these compounds.

Table 9. Arrhenius parameters for reactions 1 – 3 of the reaction network model

Parameter	Value
A_1	6358000 min^{-1}
E_{a1}	70.19 kJ/mol
A_2	50060 L mol^{-1} min^{-1}
E_{a2}	22.34 kJ/mol
A_3	2070000 L mol^{-1} min^{-1}
E_{a3}	28.21 kJ/mol

4 Conclusions

In summary, this work developed a first principles kinetic model for the synthesis of carbamazepine from iminostilbene and urea that was used for modeling both batch and continuous flow systems. For both kinetic models, a good agreement between model prediction and experimental results was observed, though the developed continuous model was susceptible to overpredicting the reaction yield at higher conversions. Some data also indicated that the reverse reaction was less prevalent for continuous experiments conducted with a pre-conversion step because this step allowed the byproduct ammonia to escape into the gas phase. This hypothesis should be further explored as separating the byproduct ammonia from the reaction mixture would minimize the reverse reaction and maximize the yield. Either a series of CSTRs that are open to the air similar to the batch reactor or a tubular membrane reactor with an ammonium permeable membrane could be studied for continuous synthesis with ammonia removal. Both the existence of the reverse reaction and the ammonia escape into air were insights gained by the use of a first principles model demonstrating the value of the enhanced process understanding provided by the mechanistic model.

Acknowledgements

This project was supported in part by a fellowship appointment to the Research Participation Program at the Center for Drug Evaluation and Research administered by the Oak Ridge Institute for Science and Education (ORISE) through an agreement between the U.S. Department of Energy and FDA.

Author Contributions

According to CRediT contributions descriptions.
Harrison F. Kraus: Conceptualization, Data curation, Formal analysis, Investigation, Methodology, Software, Visualization, Writing – original draft.
David Acevedo: Conceptualization, Writing – review and editing.
Wei Wu: Methodology, Writing – review and editing.
Thomas F. O'Connor: Writing – review and editing.
Adil Mohammad: Conceptualization, Writing – review and editing, Funding acquisition, Resources.
Dongxia Liu: Conceptualization, Writing – review and editing, Methodology, Resources.

Notes and references

1. Leuenberger, H., New trends in the production of pharmaceutical granules: batch versus continuous processing. *European Journal of Pharmaceutics and Biopharmaceutics.* 2001, *52* (3), 289-296.
2. Plumb, K., Continuous processing in the pharmaceutical industry - Changing the mind set. *Chemical Engineering Research and Design.* 2005, *83* (A6), 730-738.
3. Poechlauer, P.; Manley, J.; Broxterman, R.; Gregertsen, B.; Ridemark, M., Continuous Processing in the Manufacture of Active Pharmaceutical Ingredients and Finished Dosage Forms: An Industry Perspective. *Organic Process Research & Development.* 2012, *16* (10), 1586-1590.
4. Roberge, D. M.; Zimmermann, B.; Rainone, F.; Gottsponer, M.; Eyholzer, M.; Kockmann, N., Microreactor technology and continuous processes in the fine chemical and pharmaceutical industry: Is the revolution underway? *Organic Process Research & Development.* 2008, *12* (5), 905-910.
5. Gutmann, B.; Cantillo, D.; Kappe, C. O., Continuous-Flow TechnologyA Tool for the Safe Manufacturing of Active Pharmaceutical Ingredients. *Angewandte Chemie International Edition.* 2015, *54* (23), 6688-6728.
6. Berry, M. B., Filing a Multistage Continuous Process for API. *American Pharmaceutical Review* 2020.
7. Roberge, D. M. D., Laurent; Bieler, Nikolaus; Cretton, Philippe; Zimmermann, Bertin., Microreactor Technology: A Revolution for the Fine Chemicaland Pharmaceutical Industries? *Chemical Engineering & Technology* 2005, *28* (3), 318-323.

8. Pollet, P. C., Elizabeth D.; Kassner, Michelle K.; Charney, Reagan; Terett, Stuart H.; Richman, Kent W.; Dubay, William; Stringer, Joy; Eckert, Charles A.; Liotta, Charles L., Production of (S)-1-Benzyl-3-diazo-2-oxopropylcarbamic Acid tert-Butyl Ester, a Diazoketone Pharmaceutical Intermediate, Employing a Small Scale Continuous Reactor. *Industrial & Engineering Chemistry Research.* 2009, *48*, 7032-7036.
9. Britton, J.; Raston, C. L., Multi-step continuous-flow synthesis. *Chemical Society Reviews.* 2017, *46* (5), 1250-1271.
10. Mesbah, A.; Paulson, J. A.; Lakerveld, R.; Braatz, R. D., Model Predictive Control of an Integrated Continuous Pharmaceutical Manufacturing Pilot Plant. *Organic Process Research & Development.* 2017, *21* (6), 844-854.
11. Bhaskar, A.; Barros, F. N.; Singh, R., Development and implementation of an advanced model predictive control system into continuous pharmaceutical tablet compaction process. *International Journal of Pharmaceutics.* 2017, *534* (1-2), 159-178.
12. Morari, M.; Lee, J. H., Model predictive control: past, present and future. *Computers & Chemical Engineering.* 1999, *23* (4-5), 667-682.
13. Lee, S. M., Yohihiro, Q13 Continuous Manufacturing of Drug Substance and Drug Products. Harmonisation, I. C. f., Ed. 2021.
14. Yu, L. X., Pharmaceutical quality by design: Product and process development, understanding, and control (vol 25, pg 10, 2008). *Pharmaceutical Research.* 2008, *25* (10), 2463-2463.
15. Haugen, F., *Basic Dynamics and Control*. TechTeach: 2010.
16. International Conference on Harmonization (ICH) and FDA Guidance for Industry, Q8 (R2) Pharmaceutical Development. Nov. 2009.
17. Cao, H. Y.; Mushnoori, S.; Higgins, B.; Kollipara, C.; Fermier, A.; Hausner, D.; Jha, S.; Singh, R.; Ierapetritou, M.; Ramachandran, R., A Systematic Framework for Data Management and Integration in a Continuous Pharmaceutical Manufacturing Processing Line. *Processes.* 2018, *6* (5).
18. Zhang, L.; Mao, S. R., Application of quality by design in the current drug development. *Asian Journal of Pharmaceutical Sciences.* 2017, *12* (1), 1-8.
19. Weissman, S. A.; Anderson, N. G., Design of Experiments (DoE) and Process Optimization. A Review of Recent Publications. *Organic Process Research & Development.* 2015, *19* (11), 1605-1633.
20. Yu, L. X.; Amidon, G.; Khan, M. A.; Hoag, S. W.; Polli, J.; Raju, G. K.; Woodcock, J., Understanding pharmaceutical quality by design. *American Association of Pharmaceutical Scientists Journal.* 2014, *16* (4), 771-83.
21. Grom, M.; Stavber, G.; Drnovsek, P.; Likozar, B., Modelling chemical kinetics of a complex reaction network of active pharmaceutical ingredient (API) synthesis with process optimization for benzazepine heterocyclic compound. *Chemical Engineering Journal.* 2016, *283*, 703-716.
22. Hallow, D. M.; Mudryk, B. M.; Braem, A. D.; Tabora, J. E.; Lyngberg, O. K.; Bergum, J. S.; Rossano, L. T.; Tummala, S., An Example of Utilizing Mechanistic and Empirical Modeling in Quality by Design. *Journal of Pharmaceutical Innovation.* 2010, *5* (4), 193-203.
23. Armstrong, C. T.; Pritchard, C. Q.; Cook, D. W.; Ibrahim, M.; Desai, B. K.; Whitham, P. J.; Marquardt, B. J.; Chen, Y. Z.; Zoueu, J. T.; Bortner, M. J.; Roper, T. D., Continuous flow synthesis of a pharmaceutical intermediate: a computational fluid dynamics approach. *Reaction Chemistry & Engineering.* 2019, *4* (3), 634-642.
24. Burt, J. L.; Braem, A. D.; Ramirez, A.; Mudryk, B.; Rossano, L.; Tummala, S., Model-Guided Design Space Development for a Drug Substance Manufacturing Process. *Journal of Pharmaceutical Innovation.* 2011, *6* (3), 181-192.
25. Nunn, C.; DiPietro, A.; Hodnett, N.; Sun, P.; Wells, K. M., High-Throughput Automated Design of Experiment (DoE) and Kinetic Modeling to Aid in Process Development of an API. *Organic Process Research & Development.* 2018, *22* (1), 54-61.
26. Montes, F. C. C.; Gernaey, K.; Sin, G., Dynamic Plantwide Modeling, Uncertainty, and Sensitivity Analysis of a Pharmaceutical Upstream Synthesis: Ibuprofen Case Study. *Industrial & Engineering Chemistry Research.* 2018, *57* (30), 10026-10037.
27. Fath, V.; Kockmann, N.; Röder, T., In Situ Reaction Monitoring of Unstable Lithiated Intermediates through Inline FTIR Spectroscopy. *Chemical Engineering & Technology.* 2019, *42* (10), 2095-2104.
28. Shi, Z. Q.; Zaborenko, N.; Reed, D. E., Latent Variables-Based Process Modeling of a Continuous Hydrogenation Reaction in API Synthesis of Small Molecules. *Journal of Pharmaceutical Innovation.* 2013, *8* (1), 1-10.
29. Dong, Y.; Georgakis, C.; Santos-Marques, J.; Du, J., Dynamic response surface methodology using Lasso regression for organic pharmaceutical synthesis. *Frontiers of Chemical Science and Engineering.* 2022, *16* (2), 221-236.
30. Carbamazepine. https://medlineplus.gov/druginfo/meds/a682237.html (accessed December 16).
31. Carbamazepine Market Size, Share, Growth, Sales, Trade, Shipment, Export Value And Volume With Sales And Pricing Forecast By 2025. . https://www.tmrresearch.com/carbamazepine-market.
32. Eckardt, R. J., H. Process for Producing Carbamazepine. March 21, 2006.
33. Vyas, K. D. J., W. S., Kulkarni, A. K. Process for Preparing Carbamazepine from Iminostilbene. June 12, 2001.
34. Schindler, W. New n-heterocyclic compounds. August 9 , 1960.
35. Roehnert, H.; Cartens, E. 5-carbamoyl-iminodibenzyls and iminostilbenes prepn - with anticonvulsant, muscle relaxant and sedative-tranquilizing props. October 5, 1973.
36. Aufderhaar, E.; Sprecher, K.; Zergenyi, J. Process for preparing 5-cyano-5H-debenz(b,f)azepine and 5H-dibenz(b,f)azepine-5-carboxamide. May 27, 1981.
37. Aklin, G.; Aufderhaar, E.; Kaupp, G.; Raz, B.; Vogel, U. Method for preparing N,N-(dibenzohexatrienylene) ureas. January 21, 1988.
38. Ravinder, B.; Reddy, S. R.; Sridhar, M.; Mohan, M. M.; Srinivas, K.; Reddy, A. P.; Bandichhor, R., An efficient synthesis for eslicarbazepine acetate, oxcarbazepine, and carbamazepine. *Tetrahedron Letters.* 2013, *54* (22), 2841-2844.
39. Vogel, A. I., *Practical Organic Chemistry*. 5 ed.; John Miley & Sons, Inc.: New York, 1989.
40. Wang, D. D., Ning; Niu, Yanqing; Hui, Shien, A Review of Urea Pyrolysis to Produce NH3 Used for NOx Removal. *Journal of Chemistry.* 2019.
41. Dalmo, J., Westberg, E., Barregard, L. et al. Evaluation of retinol binding protein 4 and carbamoylated haemoglobin as potential renal toxicity biomarkers in adult mice treated with 177Lu-octreotate. EJNMMI Res 4, 59 (2014).